Evaporative cooling of trapped fermionic atoms

W. Geist, A. Idrizbegovic, M. Marinescu, T. A. B. Kennedy, and L. You

School of Physics, Georgia Institute of Technology, Atlanta, Georgia 30332-0430

We propose an efficient mechanism for the evaporative cooling of trapped fermions directly into quantum degeneracy. Our idea is based on an electric field induced elastic interaction between trapped atoms in spin symmetric states. We discuss some novel general features of fermionic evaporative cooling and present numerical studies demonstrating the feasibility for the cooling of alkali-metal fermionic species ^{6}Li, ^{40}K, and ^{82,84,86}Rb. We also discuss the sympathetic cooling of fermionic hyperfine spin mixtures, including the effects of anisotropic interactions.

PACS number(s): 32.80.Pj, 05.30.Jp, 03.75.Fi, 51.10.+y

I. INTRODUCTION

The success of atomic Bose-Einstein condensation (BEC) has opened a major research area [1–3] in weakly interacting quantum gases [4]. Experimental breakthroughs have been achieved thanks to several remarkable advances in atomic, molecular, and optical physics, in particular, the laser cooling and trapping of neutral particles [5,6], and the ingenious application of the evaporative cooling technique [7–9].

Evaporative cooling was first developed for magnetically confined atomic H [7], and is based on a simple principle seen in everyday life [8,9]. In a quasiequilibrium system the particles most likely to evaporate are the most energetic. In doing so, the particle leaves behind a system with a lower average energy per particle, i.e., a cooled system. Less appreciated, perhaps, is that forced evaporative cooling is the key to reaching quantum degeneracy in alkali-metal systems. A sufficient condition for successful evaporative cooling is the threshold ''runaway'' requirement, when an increased collision rate is achieved despite the loss of atoms. This technique was adapted to alkali-metal atomic systems in the first generation of BEC experiments [10]. It has since been demonstrated to work over a wide range of temperatures and densities, and has been applied to all successful BEC experiments thus far [4].

With such a powerful technique one may ask why it has not yet been used to create degenerate atomic Fermi gases. A careful examination of current magnetic trapping set-ups helps to clarify the fundamental problem. Alkali-metal atoms have two degenerate manifolds of hyperfine ground states $f = I \pm 1/2$, due to the coupling between the nuclear $\vec{I}$ and electronic spin $\vec{s}$ ($s = 1/2$). A typical magnetic trap arrangement confines the low field seeking Zeeman state with maximum spin polarization $m_f = f$ (at the moment we assume a single m_f value is trapped, mixtures of two different m_f values will be discussed later). Eigenstates of $\vec{F}^2$, where $\vec{F} = \vec{f} + \vec{f}$ is the total hyperfine spin of two colliding atoms, have definite spin exchange symmetry given by $(-1)^{2f-F} = +1$. Thus only the partial waves for which the relative orbital angular momentum l is odd contribute to the antisymmetrized scattering amplitude. From low energy atomic collision theory, we know that the partial wave phase shifts are $\delta_l(k) \propto k^{2l+1}$ for a short ranged potential, typical of alkali-

metal atoms in their ground state. Therefore only the s wave ($l = 0$) has a nonzero contribution in the low energy ($k \rightarrow 0$) limit, characterized by a scattering length $a_{sc} = -\lim_{k \rightarrow 0} \delta_0(k)/k$. One then obtains the elastic cross section $\sigma_B = 8 \pi a_{sc}^2$ for bosons, while for fermions $\sigma_F \rightarrow 0$, in the limit $k \rightarrow 0$. Without the thermal equilibration produced by elastic collisions, evaporative cooling cannot be directly applied to a single fermionic species. This is the same fundamental reason that BCS states for trapped fermionic gases are not easily accessible [11,12]. Obviously, if two or more spin components are simultaneously trapped, spin statistics does not prohibit s-wave collisions between the spins at low energy, so that sympathetic cooling is in principle possible.

In this paper we discuss an efficient mechanism for the evaporative cooling of trapped fermions. The mechanism employs an external electric field to polarize atoms, enabling cooling at low energy. We also discuss the sympathetic cooling of fermionic mixtures. The paper is organized as follows. In Sec. II we begin with a discussion of the major results for collisions between atoms in an external electric field [13]. We then outline our proposal for the evaporation kinetics of fermions, closely following the approach developed in [14,15] for bosons. We present our numerical studies and estimate the time scales for fermionic species ^{6}Li and ^{40}K. In Sec. III we discuss sympathetic cooling of fermionic spin mixtures, along the lines of the JILA experiment [16]. Finally, in Sec. IV we present our conclusions.

II. COLLISION KINETICS OF ATOMS IN AN ELECTRIC FIELD

As shown in detail in Ref. [13], polarized atoms in an external electric field interact through the dipole interaction

$$V_E(R) = -\frac{C_E}{R^3} P_2(\cos \theta), \qquad (1)$$

in addition to the usual interatomic potentials. Here, $C_E = 2E^2 \alpha_1^A(0) \alpha_1^B(0)$ is the electric field induced dipole interaction coefficient and $\alpha_1^{A,B}(0)$ are the static atomic dipole polarizabilities of the two atoms denoted by A and B, respectively. The angle between the directions of the electric field (of amplitude E) and the internuclear axis is denoted by θ,

and P_2 is the Legendre polynomial of order 2. The presence of this anisotropic interaction term completely changes the low energy collision physics. In particular, *all* partial waves now contribute to the low energy scattering cross sections since one can prove analytically that $\delta_l(k) \sim k$ for all l [13]. The unsymmetrized low energy scattering amplitude is

$$F(\vec{k}, \hat{R}) = 4\pi \sum_{lm,l'm'} t^{l'm'}_{lm}(k) Y^*_{l'm'}(\hat{k}) Y_{lm}(\hat{R}), \qquad (2)$$

where $t^{l'm'}_{lm}$ are the reduced *T*-matrix elements, the multichannel analogs of the scattering length. Here the incident relative momentum of the two colliding atoms is denoted by $\vec{k} = k\hat{k}$, and $\vec{k}' = k\hat{R}$ is the relative momentum after the collision.

For a gas of atoms in an electric field we can now derive the collision integral for the quantum Boltzmann equation (QBE). The QBE is given by

$$\left(\frac{\partial}{\partial t} + \frac{\vec{p}}{m} \cdot \vec{\nabla}_{\vec{r}} - \vec{\nabla}_{\vec{r}} U(\vec{r}) \cdot \vec{\nabla}_{\vec{p}} \right) f(\vec{r}, \vec{p}, t) = \mathcal{I}(\vec{r}, \vec{p}, t), \qquad (3)$$

where $f(\vec{r}, \vec{p}, t)$ is the phase-space distribution function, and $U(\vec{r})$ the external trapping potential. Using Eq. (2) we arrive at the following collision integral:

$$\mathcal{I}(\vec{r}, \vec{p}_4, t) = \frac{2}{m(2\pi\hbar)^3} \int d\vec{p}_3 d\hat{q}'$$

$$\times \left| F_{B/F}\left(\frac{1}{2}(\vec{p}_3 - \vec{p}_4), \frac{1}{2}(\vec{p}_1 - \vec{p}_2) \right) \right|^2$$

$$\times \left| \frac{\vec{p}_3 - \vec{p}_4}{2} \right| \{ f(\vec{r}, \vec{p}_1) f(\vec{r}, \vec{p}_2) [1 + \eta f(\vec{r}, \vec{p}_3)]$$

$$\times [1 + \eta f(\vec{r}, \vec{p}_4)] - [1 + \eta f(\vec{r}, \vec{p}_1)]$$

$$\times [1 + \eta f(\vec{r}, \vec{p}_2)] f(\vec{r}, \vec{p}_3) f(\vec{r}, \vec{p}_4) \}, \qquad (4)$$

where F_ϕ is the symmetrized, unsymmetrized, or the antisymmetrized scattering amplitude for bosonic ($\eta = 1$), classical ($\eta = 0$), or fermionic atoms ($\eta = -1$), respectively. We have used the following notation. Two atoms with incoming momentum $\vec{p}_3$ and $\vec{p}_4$ collide and produce an outgoing pair with momentum $\vec{p}_1$ and $\vec{p}_2$. The scattering amplitude from an initial relative momentum $\vec{q} = (\vec{p}_3 - \vec{p}_4)/2$ to a final momentum $\vec{q}' = (\vec{p}_1 - \vec{p}_2)/2$ is given by $F(\vec{q}, \vec{q}')$. For elastic collisions one has $q = q'$ in addition to the conservation of the total momentum $\vec{P} = \vec{p}_3 + \vec{p}_4 = \vec{p}_1 + \vec{p}_2$ [assuming the collision to be localized in space at a fixed $U(\vec{r})$] and energy $\epsilon_3 + \epsilon_4 = \epsilon_1 + \epsilon_2$. The differential cross section for scattering into the (relative) solid angle $d\hat{q}'$ is given by $d\sigma = |F(\vec{q}, \vec{q}')|^2 d\hat{q}'$, and $|F(\vec{q}, \vec{q}')|^2 = |F(\hat{q}, \hat{q}, ')|^2$ for the low energy collisions under consideration. The approximation of

localized collisions within a small spatial region compared with the variations of $U(\vec{r})$ allows us to neglect the $\vec{P}$ dependence of F.

Assuming an ergodic distribution for the system, we introduce the energy dependent single particle distribution function $n(\epsilon, t)$ and obtain the kinetic equation in ergodic approximation [14],

$$\rho(\epsilon_4) \frac{\partial}{\partial t} n(\epsilon_4, t) \approx \frac{m\sigma_\phi}{\pi^2\hbar^3} \int d\epsilon_1 d\epsilon_2 d\epsilon_3 \delta(\epsilon_1 + \epsilon_2 - \epsilon_3 - \epsilon_4)$$

$$\times \rho(\min[\epsilon_1, \epsilon_2, \epsilon_3, \epsilon_4]) \{ n(\epsilon_1) n(\epsilon_2) [1$$

$$+ \eta n(\epsilon_3)] [1 + \eta n(\epsilon_4)] - [1 + \eta n(\epsilon_1)] [1$$

$$+ \eta n(\epsilon_2)] n(\epsilon_3) n(\epsilon_4) \}, \qquad (5)$$

where $\rho(\epsilon)$ is the density of states. Our result is formally similar to the standard result for isotropic *s*-wave collisions in the absence of an electric field [14,15], when the *s*-wave collision cross section is replaced by the effective scattering cross sections σ_ϕ. In reaching the form of Eq. (5), the collision integral has been approximated by assuming that the fast varying part in the $\cos \theta_{\vec{q}}$ and $\cos \theta_{\vec{q}'}$ integration comes from the delta functions $\delta[\epsilon - p_i^2/2m - U(r)]$ rather than the scattering amplitude F_ϕ, thus we have extracted the scattering cross section factor out of the integrand, and replaced it by its average

$$\int d\hat{q}' d\hat{q} \frac{1}{4\pi} |F(\hat{q}, \hat{q}')|^2 = 2 \times 4\pi \sum_{lm,l'm'}^{l,l' \text{ even/odd}} |t^{l'm'}_{lm}|^2 \equiv \sigma_\eta, \qquad (6)$$

where the additional factor of 2 occurs in the Bose-Fermi case due to the symmetrization/antisymmetrization. A specific discussion of *p*-wave scattering is presented later.

For highly confined atoms inside magnetic traps, corrections due to discrete level structure need to be included. When a long range type of potential (1) is involved, one cannot in general approximate the atom-atom interaction potential by a contact $\delta(\vec{r} - \vec{r}')$ form as is usually adopted in the *s*-wave collision models. Special care is needed to find the scattering matrix element for atoms in different trap states. The quantum kinetic equation now takes the form (for bosons and fermions)

$$\frac{dn_{\vec{i}}}{dt} = \sum_{\vec{j}, \vec{k}, \vec{l}} \delta_{\epsilon_{\vec{i}} + \epsilon_{\vec{j}}, \epsilon_{\vec{k}} + \epsilon_{\vec{l}}} \gamma_{\vec{i}, \vec{j}; \vec{k}, \vec{l}} [n_{\vec{k}} n_{\vec{l}} (1 \pm n_{\vec{i}})(1 \pm n_{\vec{j}})$$

$$- n_{\vec{i}} n_{\vec{j}} (1 \pm n_{\vec{l}})(1 \pm n_{\vec{k}})], \qquad (7)$$

where $n_{\vec{i}} = n(\epsilon_{\vec{i}})$ is the population in level $\epsilon_{\vec{i}} = \hbar(i_x \omega_x + i_y \omega_y + i_z \omega_z)$ with ω_x, ω_y, and ω_z the trap frequencies in the *x*, *y*, and *z* directions.

For *s*-wave collisions, when the contact potential is valid, the collisional matrix element is given by

$$\gamma_{\vec{i}, \vec{j}; \vec{k}, \vec{l}} \propto \left| \int \Phi^*_{\vec{i}}(\vec{r}) \Phi^*_{\vec{j}}(\vec{r}) \Phi_{\vec{k}}(\vec{r}) \Phi_{\vec{l}}(\vec{r}) d\vec{r} \right|^2, \qquad (8)$$
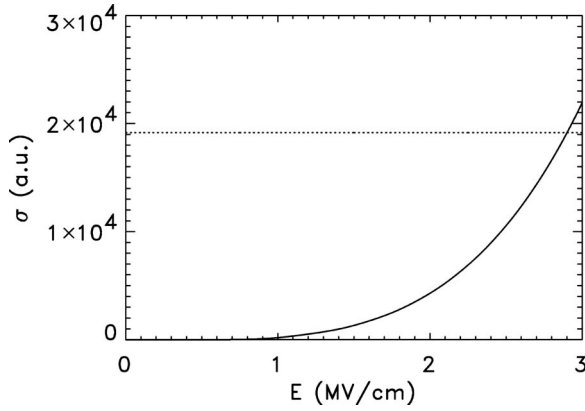
FIG. 1. The low energy collision cross section for spin triplet ^{6}Li (fermion). The dashed horizontal line indicates the field-free value of triplet ^{7}Li (boson, $a_{sc} = -27.6$ a.u.).

where $\Phi_{\vec{i}}(\vec{r})$ denotes the wave function for trap state $\vec{i} = (i_x, i_y, i_z)$. For the anisotropic collisions discussed here we have

$$\gamma_{\vec{i},\vec{j};\vec{k},\vec{l}} = \frac{2\pi}{\hbar} \frac{1}{\hbar\omega} \left| 4\pi \sum_{lm,l'm'} t_{lm}^{l'm'} \int d\vec{p}\, I_{\vec{i},\vec{j}}^{l'm'\,*}(\vec{p}) I_{\vec{k},\vec{l}}^{lm}(\vec{p}) \right|^2, \quad (9)$$

with

$$I_{\vec{i},\vec{j}}^{l'm'}(\vec{p}) = \int d\vec{q}'\, \Phi_{\vec{i}}(\vec{p}/2 + \vec{q}') \Phi_{\vec{j}}(\vec{p}/2 - \vec{q}') Y_{l'm'}^*(\hat{q}'), \quad (10)$$

where $\Phi_{\vec{i}}(\vec{p})$ is the wave function in momentum space.

Clearly, apart from final state quantum statistical factors, the collision kernel on the right-hand sides of Eqs. (5) and (7) takes the same form as that for classical atoms with s-wave collisions. For fermions, the effective cross section σ_- provides an opportunity for investigation of the ergodic kinetics as has been done previously for bosons [17,18]. Therefore the net effect of the electric field is to polarize atoms, modify their collisional properties, and thereby induce a nonzero elastic cross section at low energy. The electric field dependence of the effective cross sections $\sigma = \sigma_\pm$ allows one to control the time scale of evaporation by adjusting the strength of the electric field E. In addition, since the microscopic collision processes for polarized atoms are anisotropic, kinetic motions in different spatial directions are mixed. The validity of the ergodic approximation is thus reinforced.

Results

In this subsection we report our numerical studies of fermionic evaporative cooling in an electric field. We focus primarily on the qualitative differences between fermions and bosons in this paper, and the fundamental issues relating to fermionic evaporation. We will approximate the scattering matrix element $\gamma_{\vec{i},\vec{j};\vec{k},\vec{l}}$ by the equivalent s-wave contribution, retaining only the leading t_{00}^{00} contribution in Eq. (9). We
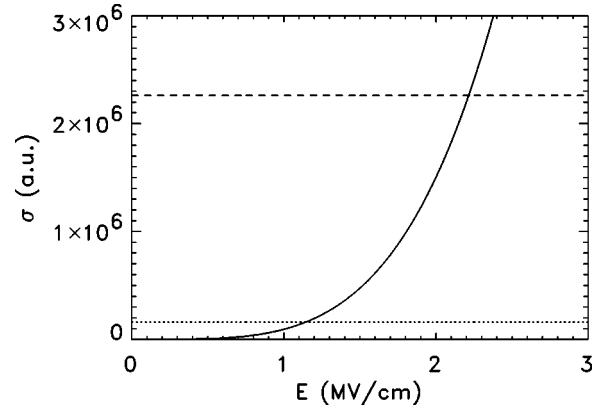

FIG. 2. The same as in Fig. 1 but for ^{40}K (fermion). The dotted line is the field-free reference value for ^{39}K (boson $a_{sc} \sim 80$ a.u.) and the dashed line the field-free reference value for ^{41}K (boson $a_{sc} \sim 300$ a.u.).

believe that this approximation should not produce any qualitative differences from the full model in the results presented.

In the early stages of evaporative cooling, when the effect of the phase-space blocking term $[1 - f(\vec{r}, \vec{p})]$ or $(1 - n_\epsilon)$ is unimportant, the kinetic term reduces precisely to that of a classical gas with an effective cross section σ_-. The evaporative kinetics of such a case have been extensively studied [8,9,14,15,17,18]. The classical runaway conditions can be achieved provided loss mechanisms are controlled. For ^{6}Li, ^{40}K, and ^{82,84,86}Rb, we have performed detailed multichannel collision calculations for atoms in an electric field. For fields of the order of a few MV/cm we find that one can readily induce an effective scattering cross section as large as for their bosonic counterparts ^{7}Li, ^{39}K, ^{41}K, ^{85}Rb, and ^{87}Rb. Our results are displayed in Figs. 1, 2, and 3. The case of ^{6}Li is particularly interesting, since the triplet scattering cross section reaches the field-free value of bosonic ^{7}Li ($8\pi a_T^2$) with $a_T = -27.6$ a.u. at a value of $E \sim 3$ MV/cm [3]. For ^{40}K, it reaches the field-free bosonic isotope value of $a_T \sim 80$ a.u. for ^{39}K and $a_T \sim 300$ a.u. [19] for ^{41}K at values of
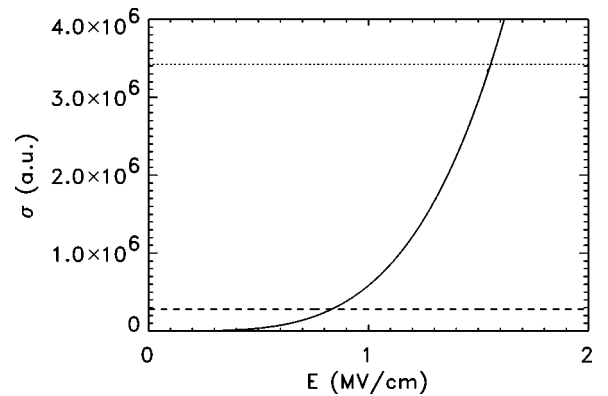

FIG. 3. The same as in Fig. 1 but for ^{86}Rb (fermion) which is similar to the results of ^{82}Rb and ^{84}Rb. The dotted line is the field-free reference value for ^{85}Rb (boson, $a_{sc} \sim 369$ a.u.) and the dashed line the field-free reference value for ^{87}Rb (boson, $a_{sc} \sim 106$ a.u.).
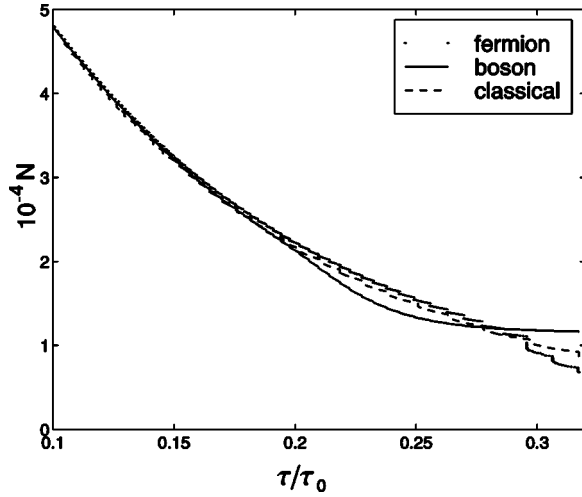
FIG. 4. Comparisons of the evaporative cooling for bosons, fermions, and classical atoms. The remaining number of atoms in the trap. The steps in the number of fermions for larger times is due to cutting discrete energies for a distribution function which does not rethermalize fast enough.

$E \sim 2$ MV/cm and $E \sim 1$ MV/cm, respectively. For ^{82,84,86}Rb, it reaches the field-free bosonic isotope value of $a_T \sim 369$ a.u. for ^{85}Rb and $a_T \sim 106$ a.u. for ^{87}Rb [20] at values of $E \sim 0.8$ MV/cm and $E \sim 1.5$ MV/cm, respectively.

The promising scenario discussed above cannot be simply extrapolated to the regime of quantum degeneracy. The effect of phase-space blocking significantly reduces the collision rates at quantum degeneracy. Time scales for evaporation are greatly prolonged for fermions, while for bosons the final state stimulation factor $(1 + n_\epsilon)$ further enhances the classical run-away evaporation. Of course this type of slowing is not unique to our scheme of fermionic evaporation, it is a generic feature of fermionic quantum statistics. As such, it is also present for other fermionic cooling schemes such as sympathetic cooling with bosons. One should realize that in this regime of phase-space density the energy scale involved
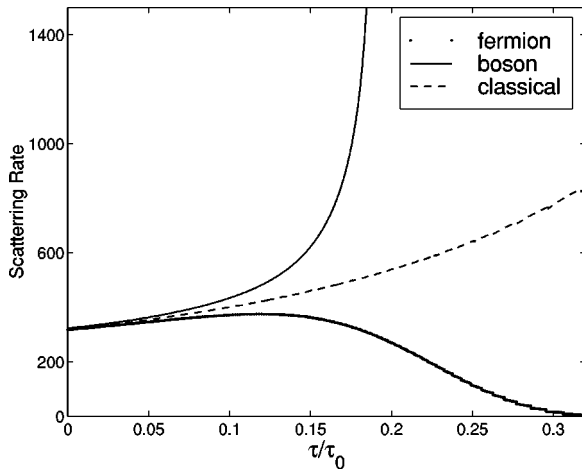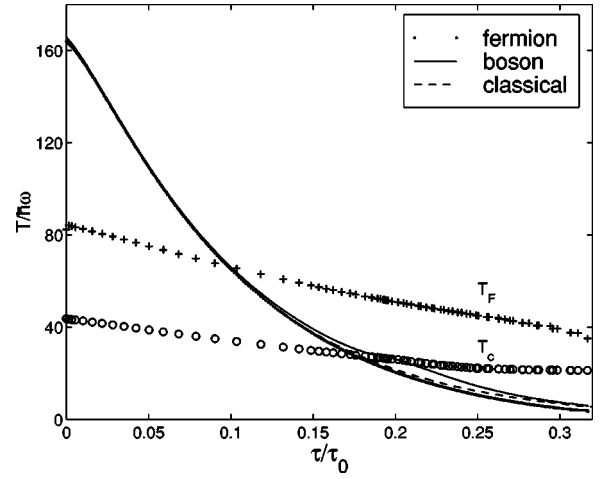

FIG. 6. The same as in Fig. 4, but for the fitted temperatures of the remaining atomic distributions.

is already extremely low, and the crucial challenge is in keeping the inelastic collision and loss rates down.

In numerical studies with Eq. (7) for a variety for parameters, we have found that down to the limit of a trapped gas temperature of the order of the Fermi energy μ_F (typically $\sim 0.5 \mu_F$), the evaporation proceeds as if the atoms were classical or bosonic, i.e., the final state blocking effect is unimportant. In Figs. 4 and 5 we display comparisons of evaporative cooling for bosons, fermions, and classical atoms (with the same collision cross section σ) contained in an isotropic harmonic trap with trap frequency $\hbar \omega$. The system contains $N = 10^5$ atoms initially, which are assumed to obey the Maxwell-Boltzmann distributions with an initial temperature $T = 164.92(\hbar \omega) = 2 T_F$, i.e., twice the initial Fermi temperature. The evaporation is effected by ramping down the trapping potential with a cut $\epsilon_{\text{cut}}(t) = \epsilon_0 e^{-\gamma_{\text{cut}} t}$. The time scale of the evaporation is $\tau = t/\tau_0$ with $1/\tau_0 \equiv (m \sigma / \pi^2 \hbar^3)(\hbar \omega)^2$. The evaporation rate is $\gamma_{\text{cut}} = \gamma_{\text{coll}}(0)/30$, with $\gamma_{\text{coll}}(0)$ the initial collision rate. The time dependent collision rate is given by
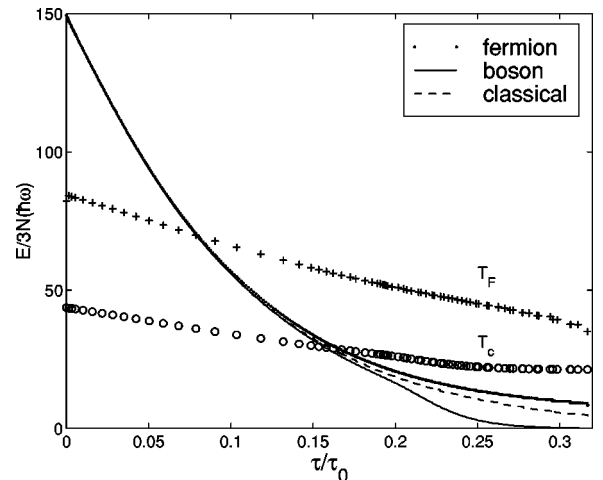

FIG. 5. The same as in Fig. 4, but for the numerically computed collision rate.

FIG. 7. The same as in Fig. 4, but for the average energy.

$$\gamma_{\text{coll}}(t) = \frac{1}{N(t)} \sum_{\epsilon_{\vec{i}}, \epsilon_{\vec{j}}, \epsilon_{\vec{k}}, \epsilon_{\vec{l}}} \delta_{\epsilon_{\vec{i}} + \epsilon_{\vec{j}}, \epsilon_{\vec{k}} + \epsilon_{\vec{l}}} \gamma(\epsilon_{\vec{i}}, \epsilon_{\vec{j}}, \epsilon_{\vec{k}}, \epsilon_{\vec{l}})$$

$$\times \{ [n_{\epsilon_{\vec{k}}}(t) n_{\epsilon_{\vec{l}}}(t)][1 + \eta n_{\epsilon_{\vec{j}}}(t)][1 + \eta n_{\epsilon_{\vec{i}}}(t)]$$

$$- n_{\epsilon_{\vec{i}}}(t) n_{\epsilon_{\vec{j}}}(t)[1 + \eta n_{\epsilon_{\vec{k}}}(t)][1 + \eta n_{\epsilon_{\vec{l}}}(t)] \}. \tag{11}$$

In Fig. 6 the temperature $T(t)$ is determined by fitting a Maxwell, Bose, or Fermi distribution function with a temperature $T(t)$ and fugacity z to the total number of remaining atoms $N(t) = \Sigma_\epsilon \rho(\epsilon) n_\epsilon [z(t), T(t)]$ and the average energy $\bar{\epsilon} = \Sigma_\epsilon \rho(\epsilon) \epsilon n_\epsilon [z(t), T(t)]$ (see also Fig. 7). In the trap, the Fermi temperature T_F and the critical temperature for Bose-Einstein condensation T_C are given by $k_B T_F = \hbar \omega (6N)^{1/3}$ and $k_B T_C = \hbar \omega (N/1.202)^{1/3}$.

III. SYMPATHETIC COOLING OF HYPERFINE FERMIONIC MIXTURES

In a recent experiment the JILA group has succeeded in implementing rf evaporation on a trapped fermionic cloud containing two spin states [16]. The effect of the low energy p-wave suppression was clearly demonstrated in their measurements of the collision rates. Our general analysis of anisotropic collisions in this paper can be adapted to an analysis of this experiment, in particular, by specializing to the case of s-wave collisions between the two trapped spin states, and p-wave collisions for each of the two spin states. We first discuss the appropriate collision integrals again assuming that trap confinement is not important during the collisions, i.e., when the ground state size of the trap is much larger than the effective range of the interatomic potential; this is true for almost all magnetic traps currently employed in laboratories. The scattering cross section

$$|F_{B/F}(\vec{q}, \vec{q}')|^2 d\hat{q}' = \left(\frac{d\sigma(\vec{q}, \vec{q}')}{d\hat{q}'} \right)_{\text{lab}} d\hat{q}'_{\text{lab}} = \frac{d\sigma(\vec{q}, \vec{q}')}{d\hat{q}'} d\hat{q}' \tag{12}$$

is invariant in different reference frames, and this enables us to write the differential scattering cross section for p-wave scattering as

$$\frac{d\sigma_p}{d\hat{q}'} = \alpha q^4 \cos^2 \theta_{\hat{q}} \cos^2 \theta_{\hat{q}'}, \tag{13}$$

where θ, θ' specify the directions of the relative momentum before and after the scattering. The constant α is obtained from the experimental data [16] in terms of an equivalent s-wave scattering cross section $\sigma_p(T_0) = \sigma_s$ at a temperature T_0, i.e.,

$$\alpha \bar{q}^4 (4\pi) = \sigma_s, \tag{14}$$

where $\bar{q}^4$ is the average of q^4 taken with respect to a Boltzmann distribution. This yields

$$\alpha = \frac{\sigma_s}{15\pi} \frac{1}{(m k_B T_0)^2}. \tag{15}$$

We can then substitute Eq. (12) into Eq. (4), and integrate over the phase space $d\vec{r} d\vec{p}_4$ again using the assumption of ergodicity

$$f(\vec{r}, \vec{p}) = \int d\epsilon n(\epsilon) \delta[\epsilon - p^2/2m - U(r)], \tag{16}$$

to obtain the ergodic Boltzmann equation for the p-wave part of the scattering,

$$\rho(\epsilon_4) \frac{\partial}{\partial t} n(\epsilon_4, t) = \frac{m\sigma_s}{\pi^2 \hbar^3} \frac{1}{45 (k_B T_0)^2} \int d\epsilon_1 d\epsilon_2 d\epsilon_3 \delta(\epsilon_1 + \epsilon_2$$

$$- \epsilon_3 - \epsilon_4) \rho(\epsilon_<) \frac{3\epsilon_> - \epsilon_<}{(\epsilon_> - \epsilon_<)^3} (\epsilon_1 - \epsilon_2)^2$$

$$\times (\epsilon_3 - \epsilon_4)^2 \{ n(\epsilon_1) n(\epsilon_2)[1 + \eta n(\epsilon_3)]$$

$$\times [1 + \eta n(\epsilon_4)] - [1 + \eta n(\epsilon_1)]$$

$$\times [1 + \eta n(\epsilon_2)] n(\epsilon_3) n(\epsilon_4) \}, \tag{17}$$

where $\epsilon_>$ ($\epsilon_<$) is the largest (smallest) of the four energies ϵ_i. We see that the collisions become ineffective as soon as the energy scales become less than $k_B T_0$. To obtain a classical collision rate we substitute the Maxwell-Boltzmann distribution

$$n(\epsilon) = z^{-1} e^{-\epsilon/k_B T} \tag{18}$$

into Eq. (17), set $\eta = 0$, and replace the sums by integrals and integrate the first term on the right-hand side over ϵ_4. This yields the p-wave collision rate as

$$\gamma_p = N(t) \frac{m\sigma_s}{\pi^2 \hbar^3} (\hbar \omega)^2 \frac{I_p \bar{T}}{45 \bar{T}_0^2}, \tag{19}$$

with the scaled temperatures $\bar{T} = k_B T / \hbar \omega$ and $I_p = 5$ is the value of the fourfold integral,

$$I_p = \int dx_1 dx_2 dx_3 dx_4 \delta(x_1 + x_2 - x_3 - x_4)$$

$$\times e^{-x_1} e^{-x_2} \rho(x_<) \frac{3x_> - x_<}{(x_> - x_<)^3} (x_1 - x_2)^2 (x_3 - x_4)^2. \tag{20}$$

In comparison the total collision rate for s-wave scattering yields

$$\gamma_s = N(t) \frac{m\sigma_s}{\pi^2 \hbar^3} (\hbar \omega)^2 \frac{I_s}{\bar{T}}, \tag{21}$$

where $I_s = 0.5$ is the value of the integral similar to Eq. (20) but only with $\rho(x_<)$ in the second line. In the above all results were given for a spherically symmetric trap with trap

frequency ω. The case of anisotropic traps can be obtained by substituting ω with $(\omega_x \omega_y \omega_z)^{1/3}$.

On the other hand, the proposed p-wave collision (inside the electric field) would not experience such a slowdown. Inside a dc-electric field, the p-wave scattering has the same nonmomentum (k) dependence as for the s wave. We will now detail the treatment for a single term $F_F(\vec{q}, \vec{q}')$ $= 4\pi t_{10}^{10} Y_{10}^*(\hat{q}) Y_{10}(\hat{q}')$ in the homogeneous case. Using approaches similar to what led to Eq. (17), we obtain

$$\rho(\epsilon_4) \frac{\partial}{\partial t} n(\epsilon_4, t) = \frac{96m}{h^3} \frac{\pi}{(\hbar\omega)^3} |t_{10}^{10}|^2 \int d\epsilon_1 d\epsilon_2 d\epsilon_3$$

$$\times \delta(\epsilon_1 + \epsilon_2 - \epsilon_3 - \epsilon_4)(\sqrt{\epsilon_>} - \sqrt{\epsilon_<})^2$$

$$\times \frac{(\epsilon_1 - \epsilon_2)^2 (\epsilon_3 - \epsilon_4)^2}{(\epsilon_> - \epsilon_<)^3}$$

$$\times \int_1^b dq \frac{(1 + b^2 - q^2 - b^2/q^2)^{3/2}}{1 + b^2 - q^2}$$

$$\times \{ n(\epsilon_1) n(\epsilon_2)[1 + \eta n(\epsilon_3)][1 + \eta n(\epsilon_4)]$$

$$- [1 + \eta n(\epsilon_1)][1 + \eta n(\epsilon_2)] n(\epsilon_3) n(\epsilon_4) \},$$

$$(22)$$

where $b = (\sqrt{\epsilon_>} + \sqrt{\epsilon_>})/(\sqrt{\epsilon_>} - \sqrt{\epsilon_>})$. Although we have not been able to complete the inside integral analytically, we can immediately see that the energy dependence for the collision rate is such that a runaway evaporation is possible in the classical limit, i.e.,

$$\gamma_p^{\mathcal{E}} \sim N(t) \frac{m|t_{10}^{10}|^2}{\pi^2 \hbar^3} (\hbar\omega)^2 \frac{1}{\bar{T}}. \qquad (23)$$

We have simulated the evaporation process for the recent experiment at JILA [16]. We assume that two hyperfine states were in the same magnetic trap, and include two types of collisions: the s-wave collision between the two states and the p-wave collision within each hyperfine state as discussed above. Inelastic processes are ignored. We start with 10^7 particles in each state at an initial temperature which is 135 times the initial Fermi temperature. Then we evaporatively cool the mixture by cutting off the hot atoms (from both states) with a cut rate which is 1/20 times the initial collision rate. The atoms rethermalize via p-wave and s-wave scattering. The p-wave collision rate decreases as the temperature of the gas decreases whereas the s-wave collision rate increases due to runaway evaporative cooling down to a temperature when Fermi statistics become important and the final state blocking term $1 - n(\epsilon)$ causes the collision rate to decrease. At the end of the cooling process the temperature is more than nine times smaller than the final Fermi temperature and there are fewer than 1.3×10^6 particles left in each state. This corresponds to an increase of phase-space density of more than 10^{12}. The final average peak density in the trap is then $\bar{n} = 3.2 \times 10^{14}/\text{m}^3$.

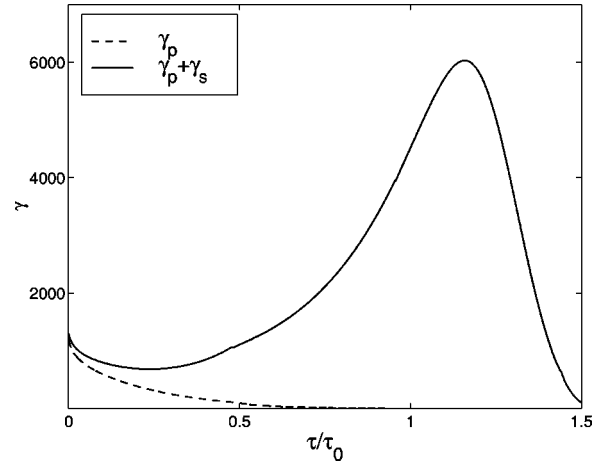In Fig. 8 we show our results for the numerically com-

FIG. 8. The numerically computed collision rates γ_p and γ_s for the discussed two state evaporation simulation.

puted collision rates. We note that the p-wave collision rate essentially dies out at the temperature measured by the JILA experiment [16]. The sum of the two scattering rates initially decreases due to the suppressed p-wave collisions, the total rate eventually increases as the runaway evaporation sets in for the s-wave scattering. We started the evaporation at an initial temperature of $\bar{T}_i = 5.23 \times 10^5$ and have used the parameters of $\sigma_s = \sigma_p = 10^{-11}$ cm^2 at $\bar{T}_0 = \bar{T}_i/4$ from the JILA results [16]. Assuming an average trap frequency of $\omega \approx (2\pi) 80$ Hz this corresponds to an initial temperature of $T_i = 200$ μK. The simulation was started with 500 energy bins and each bin covers an energy interval of $800\hbar\omega$. After the cut energy is ramped down to 40 energy bins, the energy interval is decreased by a factor of 10, a redistribution of all particle numbers to 500 finer energy bins is required. This procedure is repeated twice before one finally gets down to the required low temperature. The accuracy and convergence were checked by simulations with a larger number of energy bins. In Fig. 9 we show the temperature of the evaporated mixture as well as the corresponding Fermi temperature [computed in terms of $N(t)$ and $T(t)$]. We note that with
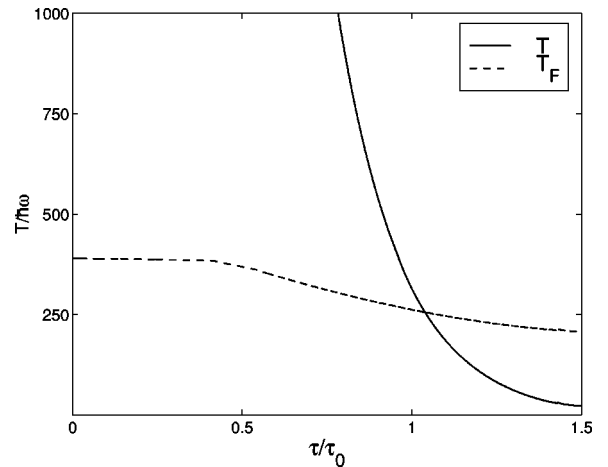

FIG. 9. The temperature and the Fermi temperature for the evaporated two state Fermi mixture.

appropriate initial conditions the gas will cross the Fermi degeneracy, at a time $t_{deg}=3.3\times10^{-3}\omega^2$ for the parameters used in the simulation, e.g., $t=\tau_0=7.95$ s for $\omega/2\pi=80$ Hz. We have not included inelastic loss processes such as three body collisions, however, as long as the inelastic loss rate G is such that $G\bar{n}^2<t_{deg}^{-1}$, the cooling process will successfully reach the degenerate regime.

IV. CONCLUSION

In conclusion, we have proposed the possibility of evaporative cooling of trapped fermionic atoms in an external electric field. We have derived effective quantum kinetic equations for fermionic atoms with anisotropic dipole-dipole interactions, and presented numerical simulations for fermionic evaporative cooling. We have also discussed sympathetic cooling of fermionic mixtures, related to a recent experiment [16], when two hyperfine states of ^{40}K are magnetically trapped. Cooling is principally due to the predominant s-wave collisions between the two states. We have observed intrastate p-wave suppression consistent with the experimental results. In the region where degeneracy becomes important we have contrasted the qualitative differences in the evaporative cooling dynamics of bosons and fermions.

[1] M.H. Anderson, J.R. Ensher, M.R. Matthews, C.E. Wieman, and E.A. Cornell, Science **269**, 198 (1995).

[2] K.B. Davis, M.-O. Mewes, M.R. Andrews, N.J. van Druten, D.S. Durfee, D.M. Kurn, and W. Ketterle, Phys. Rev. Lett. **75**, 3969 (1995).

[3] C.C. Bradley, C.A. Sackett, J.J. Tollett, and R.G. Hulet, Phys. Rev. Lett. **75**, 1687 (1995); **79**, 1170 (1997).

[4] For an extentive list of references, see the BEC on-line bibliography at Georgia Southern University: http://amo.phy.gasou.edu/bec.html/bibliography.html.

[5] See the special issue *Laser Cooling and Trapping of Atoms*, edited by S. Chu and C. E. Wieman, J. Opt. Soc. Am B **6** (1989).

[6] S. Chu, Rev. Mod. Phys. **70**, 685 (1998); C.C. Tannoudji, *ibid.* **70**, 707 (1998); W.D. Phillips, *ibid.* **70**, 721 (1998).

[7] H. Hess, G. P. Kochanski, J. M. Doyle, N. Masuhara, D. Kleppner, and T. Greytak, Phys. Rev. Lett. **59**, 672 (1987).

[8] W. Ketterle and N.J. van Druten, *Advances in Atomic, Molecular, and Optical Physics*, edited by B. Bederson and H. Walther (Academic Press, San Diego, 1996), Vol. 37, p. 181.

[9] J.T.M. Walraven, in *Quantum Dynamics of Simple Systems*, edited by G.L. Oppo, S.M. Barnett, E. Riis, and M. Wilkinson (Institute of Physics and Physical Society, London, 1996).

[10] W. Petrich, M. H. Anderson, and J. R. Ensher, Phys. Rev. Lett. **71**, 3352 (1995); K. B. Davis, M.-O. Mewes, and W. Ketterle, Appl. Phys. B **60**, 155 (1995).

[11] M. Houbiers *et al.*, Phys. Rev. A **56**, 4864 (1997).

[12] M. A. Baranov *et al.*, Pis'ma Zh. Éksp. Teor. Fiz. **64**, 273 (1996) [JETP Lett. **64**, 301 (1996)].

[13] M. Marinescu and L. You, Phys. Rev. Lett. **81**, 4596 (1998).

[14] O.J. Luiten *et al.*, Phys. Rev. A **53**, 381 (1996).

[15] Kristine Berg-Sorensen, Phys. Rev. A **55**, 1281 (1997).

[16] B. DeMarco and D.S. Jin, Phys. Rev. A **58**, R4267 (1998). Because of the inverted hyperfine ground states in ^{40}K, trapping the $m_f=7/2$ and 9/2 of the $f=9/2$ state energetically suppresses the decay due to spin exchange collisions. Recent results were presented at the workshop for Bose-Einstein condensation and degenerate Fermi gases at JILA (February, Boulder, 1999). Also see B. DeMarco, J.L. John, J.P. Burke, M. Holland, and D.S. Jin, Phys. Rev. Lett. **82**, 4208 (1999).

[17] M. Holland *et al.*, Phys. Rev. A **55**, 3670 (1996).

[18] D. Jaksch *et al.*, Phys. Rev. A **56**, 575 (1997).

[19] R. Cote, A. Dalgarno, H. Wang, and W.C. Stwalley, Phys. Rev. A **57**, R4118 (1998).

[20] J.P. Burke and J.L. Bohn, Phys. Rev. A **59**, 1303 (1998).